

## Synthesis and biological evaluation of thiobenzanilides as anticancer agents

Wan-Ping Hu,<sup>a</sup> Hsin-Su Yu,<sup>b</sup> Yan-Ren Chen,<sup>c</sup> Yi-Min Tsai,<sup>c</sup> Yin-Kai Chen,<sup>a</sup>  
Chao-Cheng Liao,<sup>c</sup> Long-Sen Chang<sup>d,e</sup> and Jeh-Jeng Wang<sup>c,d,\*</sup>

<sup>a</sup>Faculty of Biotechnology, College of Life Science, Kaohsiung Medical University, Kaohsiung, Taiwan

<sup>b</sup>Department of Dermatology, College of Medicine, Kaohsiung Medical University, Kaohsiung, Taiwan

<sup>c</sup>Faculty of Medicinal and Applied Chemistry, Kaohsiung Medical University, Kaohsiung, Taiwan

<sup>d</sup>National Sun Yat-Sen University – Kaohsiung Medical University Joint Research Center, Kaohsiung, Taiwan

<sup>e</sup>Institute of Biomedical Science, National Sun Yat-Sen University, Kaohsiung, Taiwan

Received 8 January 2008; revised 29 February 2008; accepted 1 March 2008

Available online 6 March 2008

**Abstract**—A series of novel thiobenzanilides is described. These compounds have been previously found to show strong biological activity such as antimycotic and antifungal actions. This is the first demonstration on the mechanism of the anticancer effect of thiobenzanilide agents (**4a–c**) on human melanoma A375 cells. The cytotoxic studies of compounds **4a–c** on human melanoma A375 cells indicate thiobenzanilides induced higher cytotoxicity than nitrobenzanilides (**3a–c**). In addition, DNA flow cytometric analysis shows that **4a–c** displays a significant G2/M phase arrest, which progresses to early apoptosis as detected by flow cytometry after double-staining with annexin V and propidium iodide (PI). Because cellular apoptosis is often preceded by the disruption of mitochondrial function, the assessment of mitochondrial function in **4a–c**-treated cells is worthy of investigation. Our data revealed that treatment of A375 cells with **4a–c** resulted in the loss of mitochondrial membrane potential ( $\Delta\Psi_{mt}$ ), a reduction of ATP synthesis, increased reactive oxygen species (ROS) generation, and activation of caspase-3. Thus, we suggest that **4a–c** agents are potent inducers of cell apoptosis in A375 cells.

© 2008 Elsevier Ltd. All rights reserved.

### 1. Introduction

Much attention has recently been paid to the discovery and development of new, more selective anticancer agents. Thiobenzanilides are found to show strong biological activity as antimycotic and antifungal agents.<sup>1</sup> However, other biological profiles such as antitumor action may also be involved in this complicated biological phenomenon and further investigation is needed to address this issue. The synthesis of thiobenzanilides (**4a–c**) with 4-nitrobenzyl moiety and the differently modified *N*-aryl fragment was carried out in our laboratory.

In the present study, we report the synthesis and biological evaluation of benzanilides (**3a–c**, **4a–c**). The human

melanoma cell line A375 was selected as a model, it is a highly metastasizable cell line resistant to radio- and chemo-therapy.<sup>2</sup> Meikrantz and Schlegel reported the control of cell death is linked to the cell cycle.<sup>3</sup> Cells with a defective cell cycle are more vulnerable to some anticancer agents according to numerous preclinical studies. Recently, perturbation of mitochondrial function has been shown to be a key event in the apoptotic cascade.<sup>4</sup> Anticancer drugs may damage the mitochondria by increasing the permeability of the outer mitochondrial membrane, which is associated with the collapse of mitochondrial membrane potential ( $\Delta\Psi_{mt}$ ). Disruption in  $\Delta\Psi_{mt}$  can be measured using rhodamine 123, a cationic lipophilic fluorochrome<sup>5</sup>; the extent of fluorescent dye uptake reflects the redox potential across the mitochondrial membrane.<sup>6</sup> This is because a decline in  $\Delta\Psi_{mt}$  can disturb the intracellular ATP synthesis, cause generation of reactive oxygen species (ROS), alter the mitochondrial redox ratio, and lead to caspase-3 activation, which is one of the major promoters of apoptotic effect.

**Keywords:** Thiobenzanilides; Human melanoma; Mitochondria; Apoptosis.

\* Corresponding author. Tel.: +886 7 312 1101x2275; fax: +886 7 312 5339; e-mail: [jjwang@kmu.edu.tw](mailto:jjwang@kmu.edu.tw)

The aim of this study was to investigate whether **4a–c** agents induced antiproliferation, leading to cell growth cycle perturbation, an aberrant mitochondrial function and subsequent apoptotic cell death.

## 2. Results and discussion

### 2.1. Syntheses

The thiobenzanilides (**4**) were synthesized in two steps (Scheme 1). Anilines (**1**) and 4-nitrobenzoyl chloride (**2**) were reacted in the presence of pyridine under reflux conditions to form benzanilides (**3**). In the second step, the benzanilides were converted to thiobenzanilides (**4**) with Lawesson's reagent in refluxing chlorobenzene.

### 2.2. In vitro cytotoxic effects

We evaluated the cytotoxicity of the benzanilides (**3a–c**, **4a–c**) in various human cell lines using an MTS cell proliferation assay. The activity of mitochondrial dehydrogenase enzymes, detectable by catalyzing MTS reagent, correlated with cell viability.<sup>7</sup> As shown in Table 1, thiobenzanilides (**4a–c**) were potently cytotoxic in sensitive human melanoma A375, K562 leukemia, and 293T kidney cell lines compared to that of nitrobenzanilides (**3a–c**). Because the agents **4a–c** exhibited a higher inhibitory activity on A375 cells compared to other cell lines at a concentration of 10  $\mu$ M, the A375 cells were selected as a model for further studies.

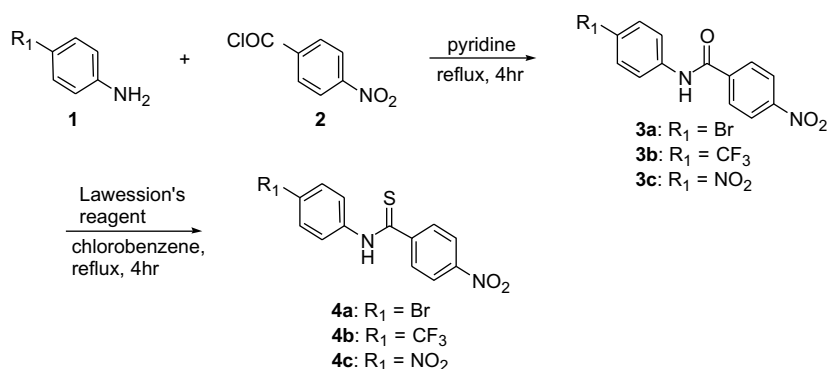
### 2.3. Cell cycle effects

To verify whether cell damage might be attributable to the cell cycle program or might have become arrested

at any cell cycle phases by **4a–c**-induced apoptosis in A375 cells, cells were treated with 10  $\mu$ M agents for 24 h. As shown in Figure 1, the majority of control cells exposed to DMSO of the cell cycle were in the G1 phase  $69.8 \pm 2.5\%$ ; S phase  $11.4 \pm 1.0\%$ , and G2/M phase  $18.8 \pm 1.6\%$ . After treatment with compounds **4a–c** for 24 h, cells progressed to the G2/M phase, and the majority of the cell population was arrested at the G2/M phase. Consistent with this cell cycle,  $58.4 \pm 0.6\%$ ,  $55.4 \pm 0.9\%$ , and  $59.9 \pm 2.5\%$  of the cells were found at the G1 phase, and  $12.7 \pm 1.1\%$ ,  $17.1 \pm 0.6\%$ , and  $11.3 \pm 0.6\%$  in S phase, with  $29.0 \pm 0.4\%$ ,  $27.6 \pm 1.5\%$ , and  $28.9 \pm 1.9\%$  in G2/M phase, respectively. Our data indicate that **4a–c** had cytotoxic effects on human melanoma A375 cells, and the cytotoxic effects may be through apoptosis induction.

### 2.4. Mitochondrial membrane potential ( $\Delta\Psi_{mt}$ ) disruption

Previous studies have suggested that a decline of  $\Delta\Psi_{mt}$  may be an early event in the process of cell death. Therefore, we investigated whether  $\Delta\Psi_{mt}$  disruption was involved in agent-induced apoptosis. A375 cells were treated with **4a–c** at a concentration of 10  $\mu$ M for 24 h, and then analyzed by flow cytometry after rhodamine 123-dye labeling. The dye binds to the inner and outer membrane of mitochondria and undergoes a red shift in fluorescence during membrane depolarization.<sup>8</sup> Compared with the untreated control group, compounds **4a–c** exhibited a marked reduction in cellular uptake of the fluorochrome (Fig. 2). The decrease of fluorescence intensity reflects the collapse of  $\Delta\Psi_{mt}$ , which generally defines an early but already irreversible stage of apoptosis.<sup>9</sup> These results reveal that exposure of melanoma A375 cells to **4a–c** inducing the drop of  $\Delta\Psi_{mt}$  may be a possible cause of the apoptotic process.



Scheme 1. Synthesis of thiobenzanilide analogs **4a–c**.

Table 1. Compounds against human-derived cancer cell lines in vitro

Survival (% control)	Compound (10 $\mu$ M)					
	3a	3b	3c	4a	4b	4c
A375 (melanoma)	$81.1 \pm 4.8$	$87.2 \pm 1.3$	$70.5 \pm 2.9$	$43.0 \pm 4.1$	$36.2 \pm 4.9$	$39.1 \pm 4.9$
K562 (leukemia)	$89.1 \pm 6.6$	$81.3 \pm 6.8$	$71.3 \pm 4.8$	$42.9 \pm 1.6$	$41.4 \pm 2.3$	$47.9 \pm 1.6$
293T (kidney)	$86.9 \pm 1.6$	$87.7 \pm 0.8$	$85.2 \pm 3.5$	$48.4 \pm 0.7$	$41.2 \pm 1.4$	$44.0 \pm 2.4$

Cells were cultured with agents at a concentration of 10  $\mu$ M for 24 h before growth and viability were assessed using the MTS cell proliferation assay.

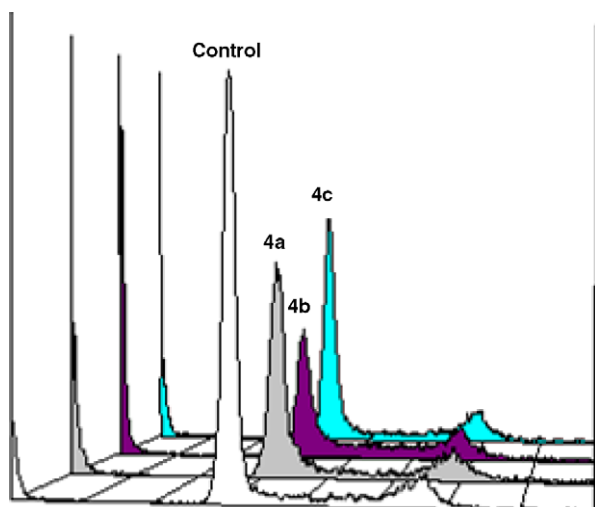


**Figure 1.** Cell cycle distribution of A375 cells after treating with compounds **4a–c**. The percentage of the cells in each phase was calculated by using the WinMDI software for the flow cytometry.

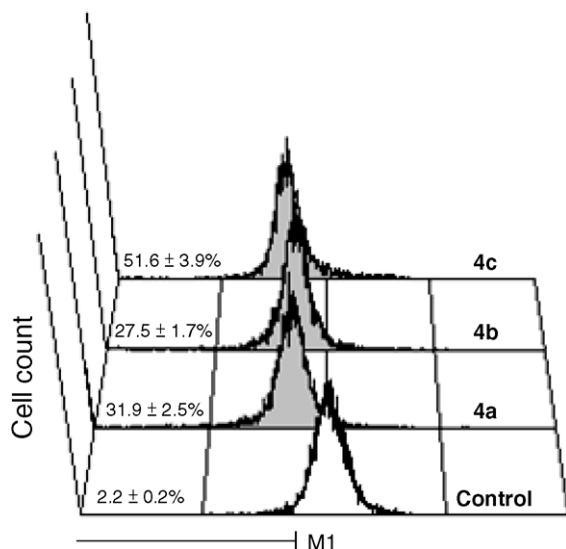


**Figure 2.** Effect of **4a–c** on the mitochondrial membrane potential ( $\Delta\Psi_{mt}$ ). Cells were cultured with different agents at a concentration of 10  $\mu\text{M}$  for 24 h, then stained with rhodamine 123 and analyzed immediately by flow cytometry as described under Section 4. The number in M1 indicates the percentage of cells with reduced  $\Delta\Psi_{mt}$ .

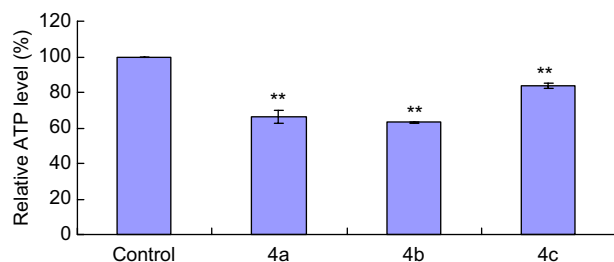


**Figure 3.** Effect of compound tested on the intracellular ATP levels. A375 cells were treated with 10  $\mu\text{M}$  agents for 24 h. Relative ATP levels were calculated as the percentage of the 0  $\mu\text{M}$  level. \*\* $p < 0.01$  as compared to the control.

## 2.5. Intracellular ATP content

ATP is the central parameter of cellular energetics, metabolic regulation, and cellular signaling; therefore, determination of intracellular ATP is worthwhile in the characterization of cellular physiology. Intracellular ATP was measured by continuously monitoring ATP production by firefly luciferase luminescence. Following exposure of cells to 10  $\mu\text{M}$  **4a–c**, the intracellular ATP content of A375 cells was  $66.1 \pm 3.8\%$  (**4a**),  $63.1 \pm 0.3\%$  (**4b**), and  $83.6 \pm 1.5\%$  (**4c**). A representative histogram is shown in Figure 3.

## 2.6. ROS generation

To determine whether ROS is involved in **4a–c**-induced apoptosis, we measured the production of intracellular  $\text{H}_2\text{O}_2$  using DCFH-DA probe. Our result showed that **4a–c** agents significantly increase intracellular  $\text{H}_2\text{O}_2$  levels. In addition, it was also observed that catalase significantly abrogated the increased ROS production of A375 cells treated with 10  $\mu\text{M}$  **4a** (Fig. 4A and B).

## 2.7. Apoptosis detection

Fluorescein isothiocyanate (FITC)-conjugated annexin V has been utilized to detect the externalization of phosphatidylserine that occurs at an early stage of apoptosis. Propidium iodide (PI) is used as a marker of necrosis due to cell membrane destruction.<sup>10</sup> To elucidate whether compound-induced cell death involved apoptosis or necrosis, we performed a biparametric cytofluorimetric analysis using annexin V and PI double-staining as shown in Figure 5. Treatment of A375 cells with 10  $\mu\text{M}$  agents for 24 h induced apoptosis effects (annexin  $\text{V}^+/\text{PI}^-$ ) in 1.7% (Control), 7.5% (**4a**), 33.0% (**4b**), and 16.3% (**4c**) of annexin V-FITC cells. Our results showed that **4a–c** agents induce more apoptotic cells than that of the untreated control; in contrast, there was no obvious change of necrotic cells (annexin  $\text{V}^+/\text{PI}^+$ ).

## 2.8. Caspase-3 activation

Caspase-3 has been shown to be one of the most important cell executioners for apoptosis.<sup>11,12</sup> The expressions of caspase-3 activity were determined using Western blotting analysis. Compared with the untreated control group, the caspase-3 activity of A375 cells increased after 10  $\mu\text{M}$  **4a–c** treatment (Fig. 6).

## 3. Conclusions

Previous reports have shown that thiobenzanilides are a promising group of compounds of a wide range of activities including antifungal and antimycotic activities. In this study, we provide evidence indicating that thiobenzanilides (**4a–c**) induce A375 melanoma cell apoptosis. This novel finding raised our interest and prompted us to elucidate the signaling mechanism of A375 cell apoptosis induced by **4a–c** treatment. First, we used an MTS cell proliferation to evaluate the cytotoxicity of tested compounds in three human cell lines, A375, K562, and

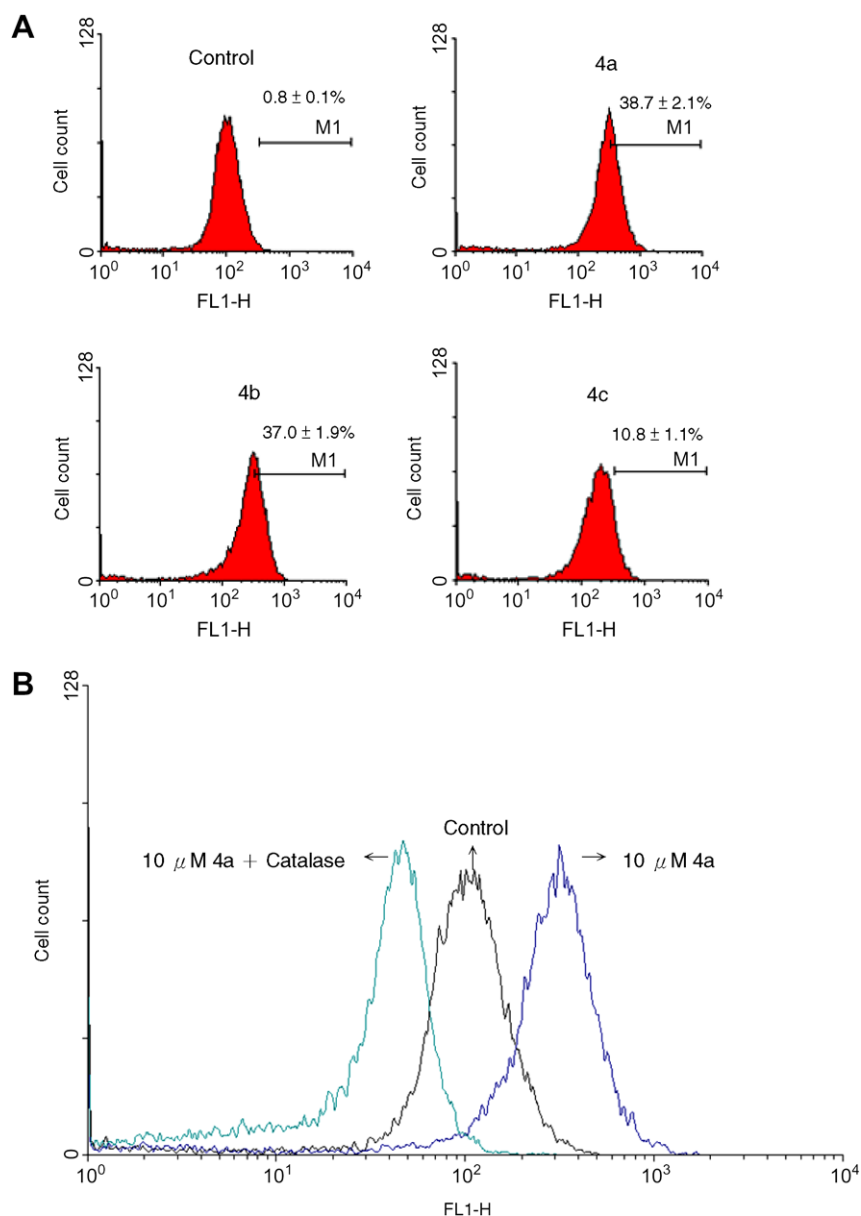


**Figure 4.** Effect of compounds **4a–c** on reactive oxygen species (ROS) generation in A375 cells. (A) Cells were untreated or incubated with 10  $\mu$ M agents for 4 h, and the ROS production (dichlorofluorescein, DCF fluorescence) was measured. (B) As a control, ROS was measured in the presence of catalase, a  $\text{H}_2\text{O}_2$  scavenger. Approximately 10,000 cells from each group were analyzed by flow cytometry. Similar results were obtained in three independent experiments.

293T. Our results indicated that **4a–c** agents are more effective as an antiproliferative agent than **3a–c**. We hypothesized that the antiproliferative effect of **4a–c** may be associated with cellular apoptosis. Because hypodiploid DNA content (sub-G1 material) is characteristic of apoptosis and reflects fragmented DNA, the sub-G1 population in A375 cells after compound treatment was measured. Our results showed that compounds **4a–c** induces more apoptotic cells than **3a–c** (data not shown). Additionally, our results also showed that **4a–c** agents induce an arrested G2/M phase and trigger apoptosis as revealed by the externalization of annexin V-targeted PS residues at the periphery of the cells.

Owing to studies suggesting that a decline of  $\Delta\Psi_{\text{mt}}$  may be an early event in the process of cell death, this prompted us to investigate whether  $\Delta\Psi_{\text{mt}}$  disruption was involved in **4a–c**-induced apoptosis. In this study, compounds **4a–c** exhibited a marked reduction in  $\Delta\Psi_{\text{mt}}$ . Mitochondrial oxidative phosphorylation is the major ATP synthetic pathway in eukaryotes. A study is in progress to investigate whether decreased intracellular ATP is due to **4a–c** treatment. Our study showed a decrease of intracellular ATP content in response to **4a–c** treatment. While mitochondria-dependent depletion of ATP would by itself damage cells due to the failure to provide energy for membrane pumps, a greater hazard is the generation of ROS. Accumulation of ROS has been

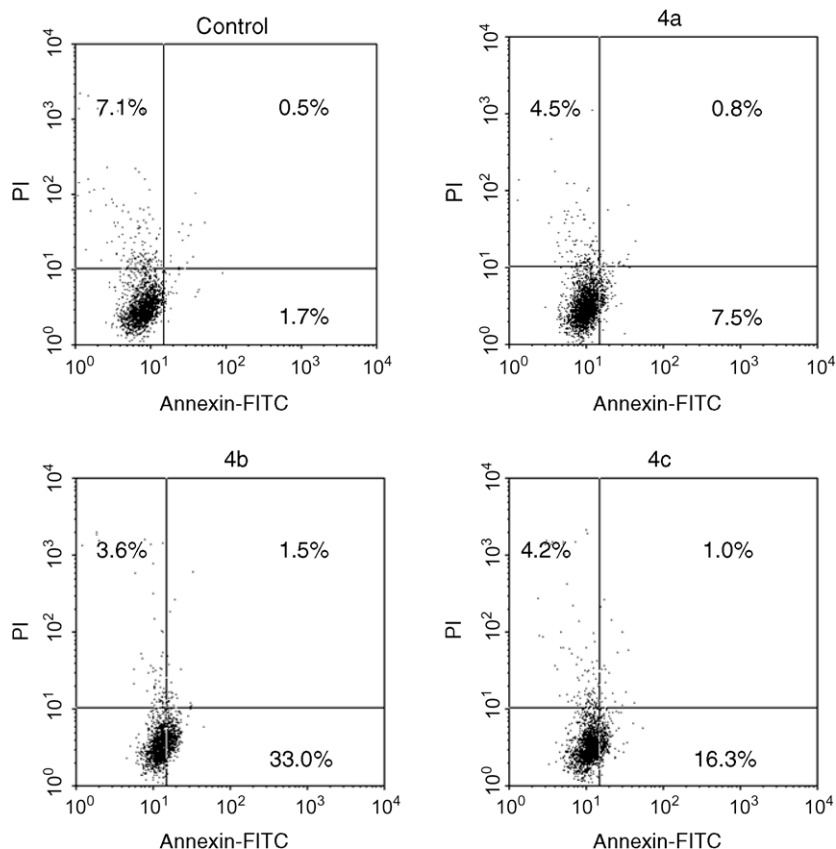


**Figure 5.** Thiobenzanilide induces externalization of PS. Dot plots for A375 cells treated with agents at a concentration of 10  $\mu$ M for 24 h and then stained with PI and an annexin V-FITC conjugate specifically detecting the exposure of PS residues at the cell surface. Approximately 10,000 cells from each group were analyzed by flow cytometry. Data shown are of a representative experiment repeated three times with similar results.

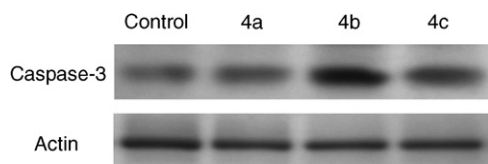


**Figure 6.** Western blot analysis showed the effect of **4a–c** treatment on activation of caspase-3. After exposure to 10  $\mu$ M **4a–c** for 24 h, cell lysates were collected and Western blotted with specific antibodies as indicated. For the internal control, the same amounts of protein extract were also probed with antibody against actin. Similar results were observed in three separate experiments.

shown to be an effective mechanism to activate programmed cell death.<sup>13</sup> We found that hydrogen peroxide ( $\text{H}_2\text{O}_2$ , a representative ROS) was involved in apoptotic effect induced by **4a–c** treatment. In addition, application of catalase, that  $\text{H}_2\text{O}_2$  scavenger, abrogated the enhanced ROS of A375 cells treated with **4a**. A recent report has shown that  $\text{H}_2\text{O}_2$ -induced cell death is predominantly a caspase-mediated apoptosis.<sup>14</sup> Caspases that are involved in the execution of apoptosis exist in living cells as inactive zymogens that become activated through intracellular caspase cascades, especially the caspase-3, which is a straight promoter of apoptosis.<sup>15,16</sup> We observed that an increase of caspase-3 activity in **4a–c**-induced A375 cells.

Based on our results, compound **4b** is the most effective one in preliminary anticancer activity. Further investigation is needed to address this issue. Our results, nevertheless, confirm for the first time that thiobenzanilides induce apoptosis in A375 cells and that thiobenzanilide-induced apoptosis may involve mitochondrial dysfunction. We expect our studies can provide an important mechanistic insight into the action of thiobenzanilides.

## 4. Experimental

### 4.1. Syntheses

$^1\text{H}$  NMR and  $^{13}\text{C}$  NMR spectra were recorded at 400 and 100 MHz, respectively. Chemical shifts are reported relative to TMS (0.0 ppm) and are designated as s (singlet), d (doublet), t (triplet). Coupling constants ( $J$  values) are reported in Hertz. Mass spectra and high resolution mass spectra (HRMS) were measured using the electron-impact (EI, 70 eV) or electron-spray-impact (ESI) technique. Flash chromatography was carried out on Silica Gel 60 (E. Merck, 230–400 mesh).

**4.1.1. General procedure for synthesis of nitrobenzamides (3).** To a stirred solution of aniline **1** (60 mmol) in pyridine (200 mL) was added 4-nitrobenzoyl chloride

(66 mmol) under nitrogen at room temperature, then the mixture was refluxed for 4 h. After being cooled to room temperature, the solution was poured into ice/water. The resulting precipitate was filtered and recrystallized from methylene chloride to give products **3**.

**4.1.1.1. *N*-(4-Bromo-phenyl)-4-nitrobenzamide (3a).** Yellow solid. Yield 17.9 g (93%). Mp 247–249 °C. <sup>1</sup>H NMR (DMSO-*d*<sub>6</sub>, 400 MHz)  $\delta$ : 10.68 (s, 1 H, NH), 8.37 (d, *J* = 8.8 Hz, 2H), 8.17 (d, *J* = 8.4 Hz, 2H), 7.76 (d, *J* = 8.4 Hz, 2H), 7.57 (d, *J* = 8.8 Hz, 2H). <sup>13</sup>C NMR (DMSO-*d*<sub>6</sub>, 100 MHz)  $\delta$ : 164.1, 149.2, 140.3, 138.1, 131.6, 129.3, 123.6, 122.4, 116.0. Anal. Calcd for C<sub>13</sub>H<sub>9</sub>BrN<sub>2</sub>O<sub>3</sub>: C, 48.62; H, 2.82; N, 8.72. Found: C, 48.58; H, 2.85; N, 8.69.

**4.1.1.2. *N*-(4-Trifluoromethyl-phenyl)-4-nitrobenzamide (3b).** Light yellow solid. Yield 17.7 g (95%). Mp 209–212 °C. <sup>1</sup>H NMR (CDCl<sub>3</sub> + DMSO-*d*<sub>6</sub>, 400 MHz)  $\delta$ : 10.30 (s, 1H, NH), 8.32 (d, *J* = 8.8 Hz, 2H), 8.20 (d, *J* = 8.8 Hz, 2H), 7.96 (d, *J* = 8.8 Hz, 2H), 7.61 (d, *J* = 8.8 Hz, 2H). <sup>13</sup>C NMR (DMSO-*d*<sub>6</sub>, 100 MHz)  $\delta$ : 164.2 (s), 149.3 (s), 141.4 (s), 140.1 (s), 128.9 (d), 125.7 (q, 31 Hz), 125.6 (q, 3.8 Hz), 123.8 (q, 270 Hz), 123.1 (d), 120.2 (d), HRMS (EI, *m/z*) for C<sub>14</sub>H<sub>9</sub>F<sub>3</sub>N<sub>2</sub>O<sub>3</sub>: calcd 310.0560; found: 310.0563.

**4.1.1.3. *N*-(4-Nitrophenyl)-4-nitrobenzamide (3c).** Light yellow solid. Yield 15.5 g (90%). Mp 267–269 °C. <sup>1</sup>H NMR (DMSO-*d*<sub>6</sub>, 400 MHz)  $\delta$ : 11.07 (s, 1H, NH), 8.37 (d, *J* = 8.8 Hz, 2H), 8.27 (d, *J* = 8.8 Hz, 2H), 8.19 (d, *J* = 8.4 Hz, 2H), 8.04 (d, *J* = 8.8 Hz, 2H). <sup>13</sup>C NMR (DMSO-*d*<sub>6</sub>, 100 MHz)  $\delta$ : 164.9, 149.6, 145.0, 143.0, 140.0, 129.6, 124.9, 123.7, 120.3. HRMS (EI, *m/z*) for C<sub>13</sub>H<sub>9</sub>N<sub>3</sub>O<sub>5</sub>: calcd 287.0542; found: 287.0542.

**4.1.2. General procedure for synthesis of thiobenzamides (4).** To a stirred solution of nitrobenzamides (**3**) (20 mmol) in chlorobenzene (20 mL) was added Lawesson's reagent (10.2 mmol) under nitrogen at room temperature, then the mixture was refluxed for 4 h. After being cooled to room temperature, hexane (60 mL) was added to the above solution. The resulting precipitate was filtered and recrystallized from acetone to give products **4**.

**4.1.2.1. *N*-(4-Bromo-phenyl)-4-nitrothiobenzamide (4a).** Orange solid. Yield 4.1 g (61%). Mp 174–177 °C. <sup>1</sup>H NMR (DMSO-*d*<sub>6</sub>, 400 MHz)  $\delta$ : 12.18 (s, 1H, NH), 8.28 (d, *J* = 8.4 Hz, 2H), 7.96 (d, *J* = 8.4 Hz, 2H), 7.78 (d, *J* = 8.8 Hz, 2H), 7.57 (d, *J* = 8.8 Hz, 2H). <sup>13</sup>C NMR (DMSO-*d*<sub>6</sub>, 100 MHz)  $\delta$ : 195.9, 148.7, 148.0, 139.1, 132.0, 129.0, 126.4, 123.8, 119.3. HRMS (ESI, *m/z*) for C<sub>13</sub>H<sub>10</sub>BrN<sub>2</sub>O<sub>2</sub>S: calcd 336.9646; found: 336.9674.

**4.1.2.2. *N*-(4-Trifluoromethyl-phenyl)-4-nitrothiobenzamide (4b).** Bright yellow solid. Yield 4.8 g (73%). Mp 182–185 °C. <sup>1</sup>H NMR (CDCl<sub>3</sub> + DMSO-*d*<sub>6</sub>, 400 MHz)  $\delta$ : 11.50 (s, 1H, NH), 8.25 (d, *J* = 8.4 Hz, 2H), 8.08 (d, *J* = 8.0 Hz, 2H), 8.00 (d, *J* = 8.4 Hz, 2H), 7.68 (d, *J* = 8.0 Hz, 2H). <sup>13</sup>C NMR (CDCl<sub>3</sub> + DMSO-*d*<sub>6</sub>,

100 MHz)  $\delta$ : 196.1 (s), 148.6 (s), 148.0 (s), 142.4 (s), 128.4 (d), 128.1 (q, 32.2 Hz), 125.8 (q, 3.2 Hz), 123.7 (q, 270 Hz), 123.5 (d), 123.2 (d). HRMS (EI, *m/z*) for C<sub>14</sub>H<sub>9</sub>F<sub>3</sub>N<sub>2</sub>O<sub>2</sub>S: calcd 326.0337; found: 326.0335.

**4.1.2.3. *N*-(4-Nitrophenyl)-4-nitrothiobenzamide (4c).** Light orange solid. Yield 3.7 g (61%). Mp: 175–178 °C. <sup>1</sup>H NMR (DMSO-*d*<sub>6</sub>, 400 MHz)  $\delta$ : 12.51 (s, 1H, NH), 8.33 (d, *J* = 8.8 Hz, 2H), 8.31 (d, *J* = 8.8 Hz, 2H), 8.22 (d, *J* = 8.8 Hz, 2H), 8.01 (d, *J* = 8.8 Hz, 2H). <sup>13</sup>C NMR (DMSO-*d*<sub>6</sub>, 100 MHz)  $\delta$ : 196.8, 148.6, 147.9, 145.3, 144.6, 128.9, 124.5, 123.9, 123.5. HRMS (EI, *m/z*) for C<sub>13</sub>H<sub>9</sub>N<sub>2</sub>O<sub>4</sub>S: calcd 303.0314; found: 303.0312.

## 4.2. Cell culture

Three human cell lines, A375 (melanoma), K562 (leukemia), and 293T (kidney), purchased from American Type Culture Collection (Manassas, VA), were maintained in DMEM (A375, 293T) or RPMI1640 (K562) medium supplemented with 10% FCS and 100 U/mL penicillin G and 100 µg/mL streptomycin sulfate (Gibco, BRL) at 37 °C in a humidified atmosphere containing 5% CO<sub>2</sub>.

## 4.3. MTS cell proliferation assay

A commercially available kit (CellTiter96 Aqueous proliferation assay kit, Promega, Madison, WI) was used to detect the proliferation according to the manufacturer's instruction. Cells were seeded in a 96-well plate at the cell density of 2500 cells/well. After an overnight incubation the **4a–c** agents at indicated concentrations was added to the culture media and incubated for 24 h. The MTS reagent contains tetrazolium salt, [3-(4,5-dimethylthiazol-2-yl)-5-(3-carboxymethoxyphenyl)-2-(4-sulfophenyl)-2H-tetrazolium], premixed with the electron coupling reagent (phenazine ethosulfate) were added into each well at 20 µL. The plate was then incubated for 1–2 h at 37 °C. The optical density value was detected by a microplate reader (MRX-II, Dynex technology, Chantilly, VA), whose detecting and reference wavelengths were set at 490 and 690 nm, respectively.

## 4.4. Cell cycle analysis

A375 cells were treated with compounds at 10 µM for 24 h. Cells were harvested by trypsinization and centrifugation. After being washed with PBS, the cells were fixed with ice-cold 70% ethanol for 30 min, washed with PBS, and then treated with 1 mg/mL of RNase A solution (containing 0.112 mg/mL of trisodium citrate) at 37 °C for 30 min. Cells were harvested by centrifugation at 400g for 5 min and further stained with 250 µL of DNA staining solution (10 mg of propidium iodide (PI), 0.1 mg of trisodium citrate, and 0.03 mL of Triton X-100 were dissolved in 100 mL H<sub>2</sub>O) at room temperature for 30 min in the dark. After loading 750 µL of PBS, the DNA contents of 10,000 events were measured by FACScan flow cytometer (Elite ESP, Beckman Coulter, Brea, CA). Histograms were analyzed using Windows Multiple Document interface software (WinMDI).



#### 4.5. Assessment of mitochondrial membrane potential ( $\Delta\Psi_{mt}$ )

A375 cells were cultured in 6-well plates and allowed to reach exponential growth for 24 h before treatment. The cells were harvested 24 h after treatment with compounds at a concentration of 10  $\mu$ M. The medium was removed and the adherent cells trypsinized. The cells were pelleted by centrifugation at 400g for 5 min and further resuspended in 1 mL of rhodamine 123 (10  $\mu$ g/mL) for 30 min at room temperature and washed with PBS twice and resuspended in PBS. The samples were analyzed for fluorescence (FL-1 detector, filter 530/30 nm band pass) by using the WinMDI software for the flow cytometry.

#### 4.6. ATP content bioluminescence assay

The amount of intracellular ATP was determined by bioluminescent assay based on the measurement of the light output of the luciferin–luciferase reaction. After treatment with **4a–c** agents at a concentration of 10  $\mu$ M for 24 h, total cell extracts from cultured A375 cells were obtained immediately by lysing methods. After centrifugation to remove cell debris, we collected supernatants for ATP measurement. The total amount of intracellular ATP was determined according to the protocol provided with the ATP lite assay kit (Perkin-Elmer, Boston, MA).

#### 4.7. Determination of intracellular ROS level

To evaluate intracellular reactive oxygen species (ROS) levels, 2',7'-dichlorofluorescein diacetate (DCFH-DA, Molecular Probes) fluorescent dye was used to clarify this issue. The nonpolar DCFH-DA is converted to the polar derivative DCFH by esterases when it is taken up by the cell. DCFH is nonfluorescent but is rapidly oxidized to the highly fluorescent DCF by intracellular  $H_2O_2$  or nitric oxide. In addition, catalase (Sigma), an effective  $H_2O_2$  scavenger, was also used in this study. Cells were pretreated with catalase (800 U/mL) before 0 and 10  $\mu$ M agents treatment. Four hours later, DCFH-DA (10  $\mu$ M) was immediately added into cultured cells for 30 min at 37 °C. The fluorescence of the samples was measured with a flow cytometer. The 2',7'-dichlorofluorescein (DCF) data were recorded using FL-1 photomultiplier.

#### 4.8. Annexin V and PI binding assay

To assess the simultaneous observation of early phase of apoptotic and necrotic features, A375 cells were treated with **4a–c** agents at a concentration of 10  $\mu$ M for 24 h, then cells were measured by cytometry by adding annexin V-FITC to  $10^6$  cells per sample according to the manufacturer's specifications (Bender MedSystems, Vienna, Austria). Simultaneously, the cells were stained with PI. Flow cytometry data were analyzed by the WinMDI software.

#### 4.9. Protein extraction and Western blot analysis

Total cell extracts from cultured A375 cells were obtained by lysing the cells in ice-cold RIPA buffer (1×

PBS, 1% NP-40, 0.5% sodium deoxycholate, and 0.1% SDS) containing 100  $\mu$ g/mL PMSF, 2  $\mu$ g/mL aprotinin, 2  $\mu$ g/mL leupeptin, and, 100  $\mu$ g/mL NaF. After centrifugation at 14,000g for 30 min, protein in the supernatants was quantified by the Bradford method (Bio-Rad). Forty micrograms of protein per lane was applied in 10% SDS–polyacrylamide gel. After electrophoresis, protein was transferred from the gel to the polyvinylidene difluoride (PVDF) membrane (Millipore, Bedford, MA). The membranes were blocked at room temperature for 1 h in PBS + 0.1% Tween 20 (PBS-T) containing 5% skim milk. After briefly rinsing with PBS-T, the membrane was incubated with primary antibody at room temperature for 2 h or at 4 °C overnight. Rabbit polyclonal antibodies against caspase-3 (p20, active form) was purchased from Santa Cruz Biotechnology. Mouse monoclonal antibody against actin was purchased from Chemicon Int. Inc. (Temecula, CA). The membrane was incubated with the corresponding horseradish peroxidase-labeled secondary antibody (Santa Cruz Biotechnology) at room temperature for 1 h. Membranes were washed with PBS-T four times for 15 min, and the protein blots were visualized with Western Lightning Chemiluminescence Reagent Plus (Perkin-Elmer Life Sciences, Boston, MA). The relative amounts of specific proteins were quantified by densitometry scanning of X-ray films and analyzed by Eagle Eye Image System (Stratagene, La Jolla, CA).

#### 4.10. Statistical analysis

All results were expressed as means values  $\pm$  standard deviation (SD) and analyzed by using the statistical analysis system (SPSS, SPSS Inc., Chicago, IL). Differences among groups were analyzed by Student's *t*-test. *P* values <0.05 were considered as significant for all statistical tests.

#### Acknowledgments

We would like to thank the National Science Council of the Republic of China, Kaohsiung Medical University Research Foundation (Q095008), and National Sun Yat-Sen University-Kaohsiung Medical University Joint Research Center for financial support.

#### Supplementary data

Supplementary data associated with this article can be found, in the online version, at [doi:10.1016/j.bmc.2008.03.003](https://doi.org/10.1016/j.bmc.2008.03.003).

#### References and notes

- (a) Matysiak, J.; Niewiadomy, A.; Macik-Niewiadomy, G. *Eur. J. Pharm. Sci.* **2000**, *10*, 119; (b) Niewiadomy, A.; Matysiak, J.; Macik-Niewiadomy, G. *Eur. J. Pharm. Sci.* **2001**, *13*, 243; (c) Waissner, K.; Kunes, J.; Odlerová, Z.; Roman, M.; Kubicová, L.; Horák, V. *Pharmazie* **1998**, *53*, 193.

2. Herlyn, M.; Clark, W. H.; Rodeck, U. *Lab. Invest.* **1987**, 56, 461.
3. Meikrantz, W.; Schlegel, R. *J. Cell Biochem.* **1995**, 58, 160.
4. Balaban, R. S. *Am. J. Physiol. Cell Physiol.* **2006**, 291, c1107.
5. Johnson, L. V.; Walsh, M. L.; Chen, L. B. *Proc. Natl. Acad. Sci. U.S.A.* **1980**, 77, 990.
6. Johnson, L. V.; Walsh, M. L.; Bockus, B. J.; Chen, L. B. *J. Cell Biol.* **1981**, 88, 526.
7. Scudiero, D. A.; Shoemaker, R. H.; Paull, K. D.; Monks, A.; Tierney, S.; Nofziger, T. H.; Currens, M. J.; Seniff, D. D.; Boyd, M. R. *Cancer Res.* **1988**, 48, 4827.
8. Scaduto, R. C.; Grotzjohann, L. W. *Biophys. J.* **1999**, 76, 469.
9. Kroemer, G.; Dallaporta, B.; Resche-Rigon, M. *Annu. Rev. Physiol.* **1998**, 60, 619.
10. Pervaiz, S.; Seyed, M.; Hirpara, J.; Clement, M.; Loh, K. *Blood* **1999**, 93, 4096.
11. Salvesen, G. S.; Dixit, V. M. *Cell* **1997**, 91, 443.
12. Shi, Y. *Mol. Cell* **2002**, 9, 459.
13. Stoian, I.; Oros, A.; Moldoveanu, E. *Biochem. Mol. Med.* **1996**, 59, 93.
14. Leung, A. M.; Redlak, M. J.; Miller, T. A. *Diq. Dis. Sci.* **2008**, PMID: 18259865.
15. Cho, S. G.; Choi, E. J. *J. Biochem. Mol. Biol.* **2002**, 35, 24.
16. Rahman, I.; Kilty, I. *Curr. Drug Targets* **2006**, 7, 707.